JCTC Journal of Chemical Theory and Computation

Karplus Equation for $^3J_{HH}$ Spin−Spin Couplings with Unusual $^3J(180°) < {}^3J(0°)$ Relationship

R. H. Contreras,[†] R. Suardíaz,[‡] C. Pérez,[‡] R. Crespo-Otero,[‡] J. San Fabián,[§] and J. M. García de la Vega*,[§]

Departamento de Física, Facultad de Ciencias Exactas y Naturales, Universidad de Buenos Aires and CONICET, Buenos Aires, Argentina, Departamento de Química Física, Facultad de Química, Universidad de la Habana, La Habana 10400, Cuba, and Departamento de Química Física Aplicada, Facultad de Ciencias, Universidad Autónoma de Madrid, 28049 Madrid, Spain

Received April 30, 2008

Abstract: Vicinal $^3J_{HH}$ coupling constants for monosubstituted ethane molecules present the unusual relationship $^3J_{HH}$ (180°) < $^3J_{HH}$ (0°) when the substituent contains bonding and antibonding orbitals with strong hyperconjugative interactions involving bond and antibond orbitals of the ethane fragment. This anomalous behavior is studied as a function of the substituent rotation for three model systems (propanal, thiopropanal, and 1-butene) at the B3LYP/TZVP level. The consistency of this level of theory to study this problem is previously established using different ab initio methods and larger basis sets. The origin of the unusual $^3J_{HH}(180°) - {}^3J_{HH}(0°)$ relationship is attributed to simultaneous σ/π hyperconjugative interactions $\sigma_{C_\alpha-H_\alpha} \rightarrow \pi^*_{C_c=X}$, and $\sigma_{C_\alpha-C_\beta} \rightarrow \pi^*_{C_c=X}$. These interactions depend on the substituent rotation and their effects are different for $^3J_{HH}(180°)$ than for $^3J_{HH}(0°)$. The modelization carried out shows an increase of those effects as the substituent changes from weaker (CH═CH_2) to stronger (CH═S) electron acceptor $\pi^*_{C=X}$.

1. Introduction

Vicinal NMR coupling constants were used extensively as stereochemical probes since Karplus pioneering works.[1,2] During the past decade, there was a renewed interest in vicinal spin−spin coupling constants (SSCC). Using these couplings as constraints in NMR structure refinement of proteins provides an important tool for increasing the definition of the peptide backbone and side chain conformations.[3]

In a previous work,[4] a valine dipeptide model was used, within the DFT framework, to obtain Karplus coefficients for $^3J_{XY}$ SSCCs whose X−C−C−Y dihedral angles are related to the dipeptide $\chi 1$ angle. It is recalled that vicinal SSCCs can be represented by a Fourier series that reduces to the usual Karplus equation[1] if the SSCC asymmetry around $\phi = 180°$ and the higher cosine terms are neglected

$$^3J_{XY}(\varphi) = C_0 + C_1\cos(\varphi) + C_2\cos(2\varphi) \qquad (1)$$

Theoretically obtained SSCCs were compared with those inferred experimentally and, in general, they show a good agreement between them.[4] The largest differences were observed for $\chi 1 = 0°$, where theoretical values were significantly larger than those obtained from empirical Karplus equations. Such theoretical couplings lead to an unusual positive coefficient C_1, eq 1, which can easily be related to the difference $^3J_{XY}(180°) - {}^3J_{XY}(0°) = -2C_1$ with $^3J_{XY}(180°) < {}^3J_{XY}(0°)$.[5] In the current literature, there are some experimental reports of positive C_1 coefficients. For instance, Chou et al.,[6] Lindorff-Larsen et al.,[7] and Juranić et al.[8] reported empirical positive C_1 coefficients for $^3J_{NC\gamma}$ in protein side chains. Positive C_1 coefficients were theoretically obtained by Case et al.[9] in valine, and by Chou et al.[6] in valine, threonine, and isoleucine. Also, $C_1 > 0$ values were reported for $^3J_{CH}$ in purine nucleotides by Munzarová et al.[10]

* Corresponding author e-mail: garcia.delavega@uam.es.
[†] Universidad de Buenos Aires and CONICET.
[‡] Universidad de la Habana.
[§] Universidad Autónoma de Madrid.

10.1021/ct800145h CCC: $40.75
Published on Web 08/14/2008

All cases mentioned above in which $C_1 > 0$ present a molecular fragment **M** bonded to the coupling pathway of the $^3J_{HH}$ SSCC. This fragment **M** contains bonding and antibonding orbitals that can undergo strong hyperconjugative interactions with the coupling pathway fragment containing the coupling nuclei X−C−C−Y (X, Y = H, H; C, H; N, H; or N, C). In every case, the Fermi contact (FC) contribution determines the C_1 sign of the respective Karplus curves. Therefore, when intending to rationalize these facts, it is of primordial importance to pay attention to the transmission mechanism of the FC term.

The FC interaction originates when the electron density probability at the site of the coupling nuclei is not null. Several features of the FC transmission, including its angular dependence when the coupling nuclei are three or more bonds apart, have been well-known for many years.[11] In recent years, a deeper insight into how the FC term is transmitted through the electronic molecular structure was achieved,[12,13] and now it is known that its transmission is closely associated to the Fermi correlation, i.e., the "same-spin electron pair density", usually known as the "Fermi hole density". This indicates that departures from the classical Lewis structures by delocalization interactions should favor the transmission of long-range SSCC. Similarly, departures from the Lewis structures could affect notably all types of SSCCs dominated by the FC term. For this reason, in this work, special attention will be paid to departures from the Lewis structures. At present, the most frequently used approach to study these departures from the Lewis scheme is the natural bond orbitals (NBO) method of Weinhold et al.,[14] which gives a description of them and provides quantitative estimations of electron delocalization interactions. Usually, these delocalization interactions are classified as conjugative and hyperconjugative interactions.

In recent works, it was shown that σ-hyperconjugative interactions play a key role in transmitting long-range SSCCs in strained saturated compounds.[15] Also, it was observed that hyperconjugative interactions affect strongly one-,[16] two-,[17] and three-bond[18] SSCCs. Recently, it was reported[19] that strong hyperconjugative interactions between bonding and antibonding orbitals are relevant to the three bond contributions to $^{3,4}J_{CH}$ and those related to the carbonyl group in norbornanones, which can affect seriously both the three- and four-bond contributions.

In a previous work,[4] we demonstrated that the main contribution to the inversion of C_1 coefficient for $^3J_{H_\alpha H_\beta}$ in aminoacids is the C═O group, whereas the NH_2 group has a weak contribution. In this work, an interpretation of the "anomalous" behavior of the Karplus type eq 1 for $^3J_{HH}$ with $C_1 > 0$ is sought in terms of the molecular electronic structure. We select the propanal (Figure 1) as a simplified model to study the relationship between hyperconjugation interactions and coupling constants. Two additional models, thiopropanal and 1-butene (Figure 1) have been used to support the conclusions obtained in the propanal and to analyze the effect of different substituents (**M** = CH═S and CH═CH_2).

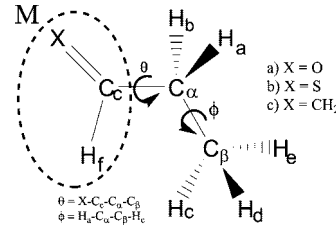

Figure 1. Propanal, thiopropanal, and 1-butene models.

2. Computational Details

Two kinds of geometries have been used in this paper. Initially, standard geometries[20] and tetrahedral angles were used for propanal to test the results of different methods and basis sets. Next, the geometries of propanal, thiopropanal and 1-butene were optimized at B3LYP/6−31G** level of theory which, is considered sufficiently accurate for the present purpose.[4,21] The geometries for the staggered (ϕ = 180°) and eclipsed (ϕ = 0°) conformers were calculated while the dihedral angle θ was varied in 30° steps from 0 to 330°. All degrees of freedom, except those of ϕ = 0° (in the eclipsed conformer) and θ, were optimized.

The 24 standard or partially optimized structures, 12 for $^3J_{HH}(180°)$ and 12 for $^3J_{HH}(0°)$, were used to calculate the four contributions to the $^3J_{HH}$: Fermi contact, spin dipolar (SD), paramagnetic spin−orbital (PSO) and diamagnetic spin−orbital (DSO). To test the quality of the results, we used the standard geometries to calculate the coupling constants of propanal with the following methods and basis set: B3LYP/TZVP, B3LYP/EPR-III, B3LYP/BS2, B3LYP/aug-cc-pVTZ-J, SOPPA/EPR-III, and CCSD(SOPPA)/EPR-III. The geometries partially optimized were used to calculate the coupling constants in propanal, thiopropanal and 1-butene at the B3LYP/TZVP level. In all studied cases, the FC term is by far the dominating one as can be appreciated with these examples for propanal (θ dihedral angle = 180°), $^3J_{HH}(180°)$ = 14.44 (FC = 15.11, SD = 0.02, PSO = 2.20, DSO = −2.89), and $^3J_{HH}(0°)$ = 13.36 (FC = 13.07, SD = 0.21, PSO = −0.18, DSO = 0.26), calculated at the B3LYP/TZVP level. NBO calculations have been performed at this same level of theory on those partial geometry optimizations. At this point, it is interesting to note that although individual hyperconjugative interactions depend on the basis set used to perform their calculations, trends of their angular dependences do not.

DFT calculations were performed with Gaussian03 software package,[22] SOPPA and CCSD(SOPPA) calculations were carried out with Dalton Software.[23] NBO 3.1[24] included in the Gaussian package[22] was used for the NBO calculations.

3. Results and Discussion

From the above considerations, it is reasonable to formulate a hypothesis connecting the peculiar features of $^3J_{HH}$ in Karplus-type equations satisfying the condition $^3J_{HH}(180°) < {}^3J_{HH}(0°)$ and hyperconjugative interactions taking place between bonding orbitals, or lone-pairs and antibonding

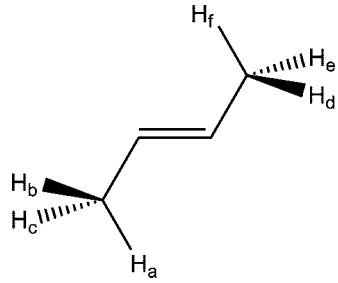

Figure 2. Homoallylic interproton coupling J_{H_b,H_e} whose coupling pathway is originated in the simultaneous existence of $\sigma_{C-H_b} \rightarrow \pi^*_{C=C}$ and $\sigma_{C-H_e} \rightarrow \pi^*_{C=C}$ σ/π hyperconjugative interactions.

orbitals of the molecular fragment **M** and those belonging to the $^3J_{HH}$ coupling pathway. In this way, propanal is taken as a model compound to elaborate a hypothesis about the influence of hyperconjugative interactions connecting the ethyl moiety with the carbonyl group (**M** fragment).

On the basis of the known[11] σ/π transmission of long-range homoallylic $^5J_{HH}$ in 2-butene, Figure 2, it can be expected that, for instance, the $^3J_{H_aH_c}$ SSCCs in propanal model of Figure 1 can be transmitted, in part, through the carbonyl π-electronic system by the simultaneous σ/π hyperconjugative interactions $\sigma_{C_\alpha-C_\beta} \rightarrow \pi^*_{C=O}$ and $\sigma_{C_\alpha-H_a} \rightarrow \pi^*_{C=O}$. It should be noted the close analogy between this assumption and the homoallylic coupling pathway shown in Figure 2. Any of these $\sigma_{C_\alpha-C_\beta} \rightarrow \pi^*_{C=O}$ and $\sigma_{C_\alpha-H_a} \rightarrow \pi^*_{C=O}$ interactions is zero whenever either the $\sigma_{C_\alpha-C_\beta}$ or $\sigma_{C_\alpha-H_a}$ bonds is contained in the carbonyl plane, i.e., for $\theta = 0$, 120, 180, and 300°. Similar effects are expected for the respective "opposite interactions", which for the sake of simplicity in this work will be called "back-donation" interactions, i.e., $\pi_{C=O} \rightarrow \sigma^*_{C_\alpha-C_\beta}$ and $\pi_{C=O} \rightarrow \sigma^*_{C_\alpha-H_a}$. It is noted that all these interactions follow either a $\sin^2\theta$ or $\sin^2\tau$ law, where θ and τ are the angles formed by the departure of the $\sigma_{C_\alpha-C_\beta}$ and $\sigma_{C_\alpha-H_a}$ bonds from the carbonyl plane, respectively. It is expected that the simultaneous occurrence of these two types of σ/π hyperconjugative interactions activates a second coupling pathway for both $^3J_{HH}(180°)$ and $^3J_{HH}(0°)$. However, the efficiency of such a σ/π coupling pathway could be different for each type of coupling and responsible for the sign inversion of C_1 coefficient.

Propanal Model. To select the functional and basis set appropriated for this work and to test the quality of the used calculations, the results from different methods and basis set are presented in Figure 3. The SSCCs for propanal have been calculated at the B3LYP functional and at the SOPPA and CCSD(SOPPA) approaches using EPR-III basis set. Although some qualitative differences are observed, for instance, the calculated values follow the relation $^3J_{HH}$ (CCSD(SOPPA)) < $^3J_{HH}$ (SOPPA) < $^3J_{HH}$ (B3LYP) independently of θ, in general, the qualitative dependence on θ is similar (see Figure 3). As regards to the differences $^3J_{HH}$ (180) − $^3J_{HH}$ (0), the ab initio methods give smaller values in magnitude but, again, the dependence on θ is similar for the three methods.

In addition, the B3LYP functional has been used with four basis sets of different size. The results for all basis sets are qualitatively similar. Moreover, the B3LYP results obtained with the smallest basis set (TZVP) yield the closest results to those of ab initio methods. This similitude between B3LYP/TZVP and ab initio/EPR-III could be attributed to a compensation between method and basis sets effects. On the other hand, B3LYP/TZVP has been recently tested successfully in the calculation of NMR coupling constants[25] and EPR hyperfine couplings.[21] Accordingly, we use B3LYP/TZVP to calculate $^3J_{HH}$ for the remaining systems presented in this work.

To quantify the hyperconjugative interaction and its effect on the SSCCs, we carried out $^3J_{HH}$ as well as NBO calculations for the propanal model. Using the notation shown in Figure 1, we calculated $^3J_{HH}(180°)$ and $^3J_{HH}(0°)$

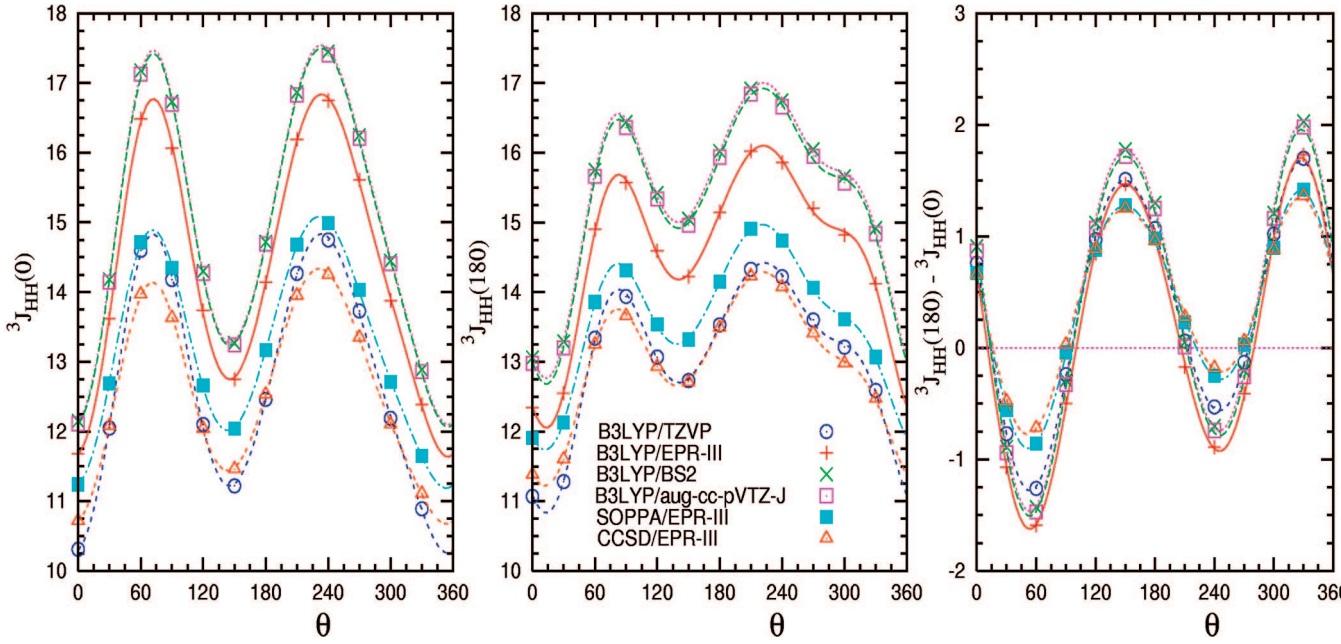

Figure 3. Ab initio and DFT calculated $^3J_{H_aH_c}(180°)$, $^3J_{H_aH_c}(0°)$, and $^3J_{H_aH_c}(180°) - {}^3J_{H_aH_c}(0°)$ differences for propanal model.

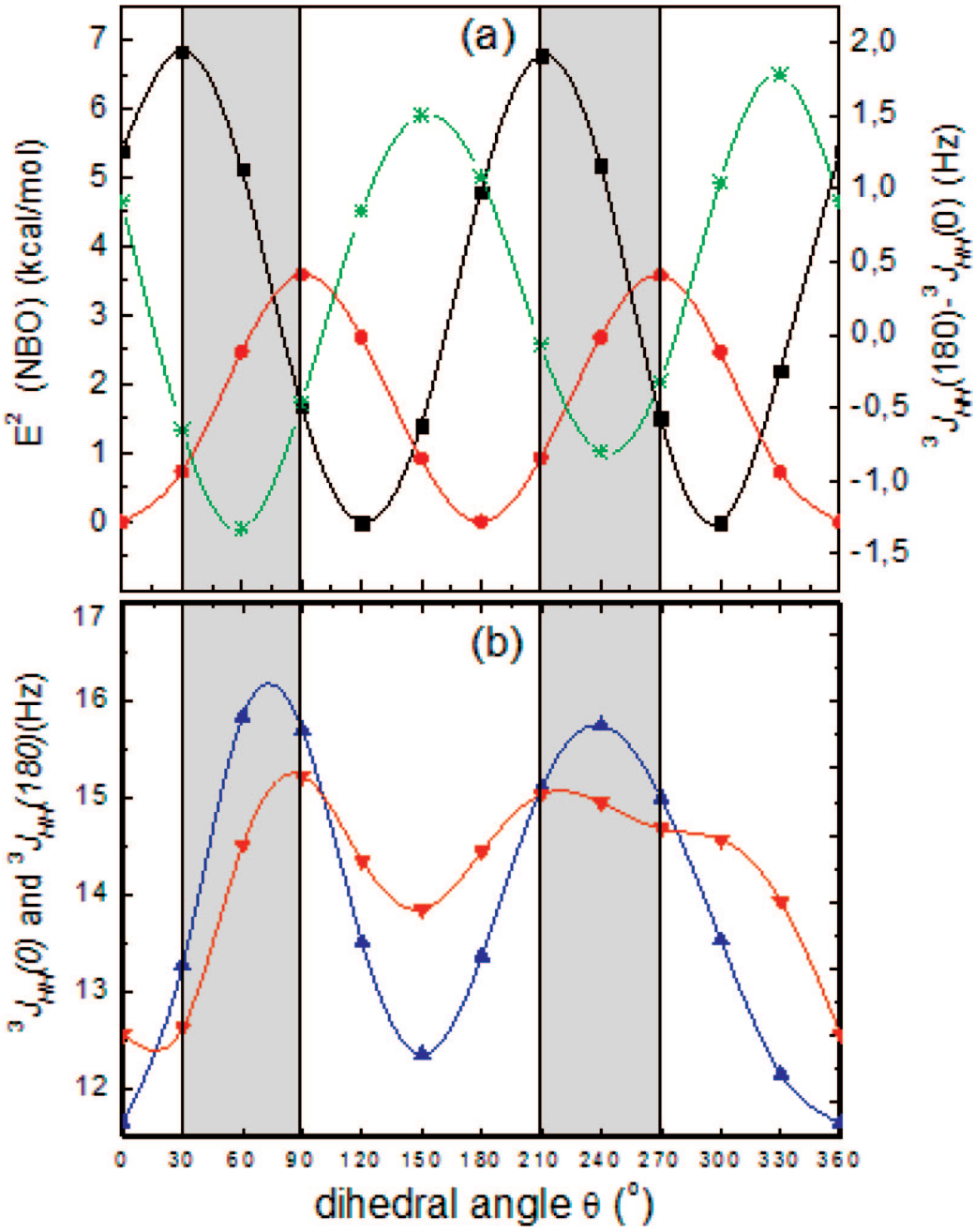

Figure 4. (a) Plots of E^2(NBO) $\sigma_{C_\alpha-C_\beta} \rightarrow \pi^*_{C=O}$ (•), $\sigma_{C_\alpha-H_a} \rightarrow \pi^*_{C=O}$ (■), and $^3J_{H_aH_c}(180°) - {}^3J_{H_aH_c}(0°)$ (*). (b) Plots of $^3J_{H_aH_c}(0°)$ (▲), and $^3J_{H_aH_c}(180°)$ (▼) vs dihedral angle θ. The zones of maxima hyperconjugation (both, $\sigma_{C_\alpha-H_a} \rightarrow \pi^*_{C_c=O}$ and $\sigma_{C_\alpha-C_\beta} \rightarrow \pi^*_{C_c=O}$) that coincide with the zones where $^3J_{HH}(180) < {}^3J_{HH}(0)$ are shaded in these plots.

for the ethyl $H_aC_\alpha-C_\beta H_c$ moiety. Both types of couplings were calculated for different rigid rotations around the C_c-C_α bond, θ angle; values for $^3J_{H_aH_c}(180°)$ were obtained taking the staggered conformation of the ethyl group, while values of $^3J_{H_aH_c}(0°)$ were obtained taking the eclipsed conformation, Figure 1. Figure 4a shows the $^3J_{H_aH_c}(180°) - {}^3J_{H_aH_c}(0°)$ difference as well as the hyperconjugative interactions $\sigma_{C_\alpha-H_a} \rightarrow \pi^*_{C_c=O}$ and $\sigma_{C_\alpha-C_\beta} \rightarrow \pi^*_{C_c=O}$ versus θ. The following features of these three plots shown in Figure 4a are worth highlighting:

(a) The values of $^3J_{HH}(0°)$ and $^3J_{HH}(180°)$ depend notably on θ, this dependence being nonsymmetric around $\theta = 180°$. This asymmetry seems to originate mainly on the proximity between the carbonyl O and the H_a atom for $\theta = 120°$ and the carbonyl O and the H_c atom for $\theta = 300°$ (the former for both the staggered and the eclipsed conformation, and the latter only for the ethyl staggered conformation).

(b) Both σ/π hyperconjugative interactions follow the well-known $\sin^2\theta$ dependence, lagging the $\sigma_{C_\alpha-C_\beta} \rightarrow \pi^*_{C_c=O}$ plot 60° with respect to that of $\sigma_{C_\alpha-H_a} \rightarrow \pi^*_{C_c=O}$.

As shown in Figure 4b, both types of couplings depend on θ angle, the sensitivity of $^3J_{HH}(0°)$ being higher than that of $^3J_{HH}(180°)$. This indicates that the "activated" coupling pathway due to the hyperconjugative interactions involving the carbonyl group shows a different efficiency for $^3J_{HH}(180°)$ and $^3J_{HH}(0°)$. In Figure 4, the zones of maxima hyperconjugation (both, $\sigma_{C_\alpha-H_a} \rightarrow \pi^*_{C_c=O}$ and $\sigma_{C_\alpha-C_\beta} \rightarrow \pi^*_{C_c=O}$), that coincide with the zones where $^3J_{HH}(180) < {}^3J_{HH}(0)$, are

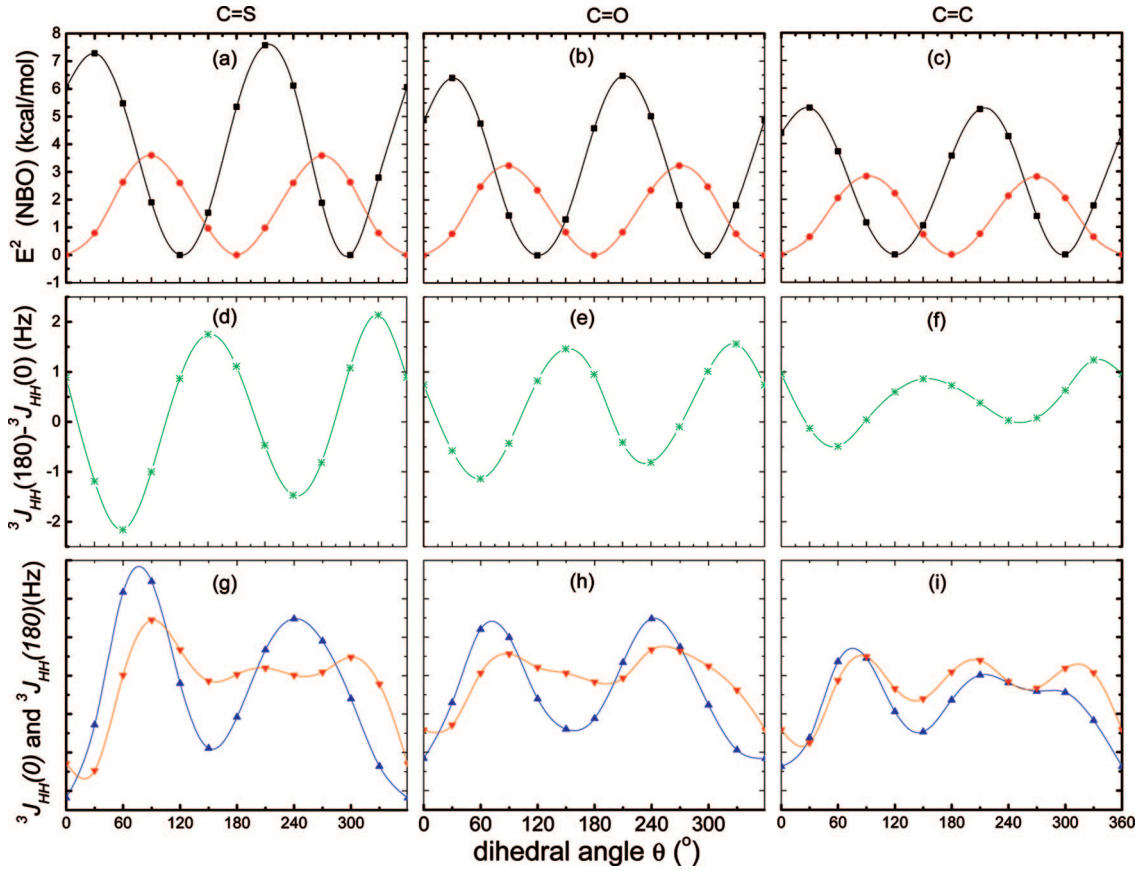

Figure 5. Plots of E^2(NBO) $\sigma_{C_\alpha-C_\beta} \rightarrow \pi^*_{C=X}$ (•) and $\sigma_{C_\alpha-H_a} \rightarrow \pi^*_{C=X}$ (■) (first row); $^3J_{H_aH_c}(180°) - {}^3J_{H_aH_c}(0°)$ (second row); and plots of $^3J_{H_aH_c}(0°)$ (▲) and $^3J_{H_aH_c}(180°)$ (▼) (third row) vs dihedral angle θ, for thiopropanal (first column), propanal (second column), and 1-butene (third column).

highlighted. Those zones correspond to an inversion of the C_1 coefficient.

For $\theta = 0$, 120, 180, and 300°, the behavior of both $^3J_{HH}(0)$ and $^3J_{HH}(180)$ SSCCs cannot be described by the σ/π hyperconjugative interactions because either $\sigma_{C_\alpha-C_\beta} \rightarrow \pi^*_{C_c=O}$ or $\sigma_{C_\alpha-H_a} \rightarrow \pi^*_{C_c=O}$ interactions are equal to zero. For these four conformers, $^3J_{HH}(180°)$ is notably larger than in $^3J_{HH}(0°)$ (about 1 Hz). It is interesting to remark that in ethane molecule, this difference, $^3J_{HH}(180) - {}^3J_{HH}(0)$, calculated at the MCSCF/RAS level, is around 0.94 Hz,[26] which is similar to that found above.

For $\theta = 240°$ the σ/π hyperconjugative interactions seem to be the main contribution to both SSCCs in defining the $^3J_{HH}(180°) - {}^3J_{HH}(0°)$ value. On the other hand, for $\theta = 270°$ the carbonyl O atom is nearing the $\sigma_{C_\beta-H_c}$ bond, the nearest approach being for $\theta = 300°$. It is observed in Figure 4b that $^3J_{H_aH_c}(180°)$ for $\theta = 300°$ is similar to $^3J_{H_aH_c}(180°)$ for $\theta = 120°$, yielding the expected conclusion that the proximity effect on $^3J_{HH}(180°)$ is similar whether either the $\sigma_{C_\alpha-H_a}$ or $\sigma_{C_\beta-H_c}$ bonds are close to the carbonyl oxygen.

It is important to remark that the coupling pathway defined by the simultaneous $\sigma_{C_\alpha-H_a} \rightarrow \pi^*_{C_c=O}$, $\sigma_{C_\alpha-C_\beta} \rightarrow \pi^*_{C_c=O}$ hyperconjugative interactions and their respective back-donations refers only to the FC term. The sum of the SD, PSO, and DSO contributions are larger in absolute value for $^3J_{HH}(180°)$ than for $^3J_{HH}(0°)$; however, the SD + PSO + DSO sum for each of them is notably insensitive to the θ angle and therefore the $^3J_{HH}(180°) - {}^3J_{HH}(0°)$ trend is by far defined by the FC term.

Thiopropanal and 1-Butene Models. The analysis presented above for propanal supports the hypothesis about the electronic origin of the $^3J_{HH}(180°) < {}^3J_{HH}(0°)$ relationship in this model system. Because hyperconjugative interactions of types $\sigma_{C_\alpha-H_a} \rightarrow \pi^*_{C_c=O}$, $\sigma_{C_\alpha-C\beta} \rightarrow \pi^*_{C_c=O}$, and their respective back-donations play the main influence on such a relationship, it is considered convenient to look for similar models where the main difference with propanal is due to σ/π interactions. For instance, if the carbonyl group in propanal is replaced by a thiocarbonyl group, Figure 1, then it is expected that the $\pi^*_{S=C}$ antibonding orbital to be a better electron acceptor than the $\pi^*_{O=C}$ antibonding orbital. Hence, in thiopropanal, the relevant σ/π interactions should be more important than in propanal. On the other hand, if in propanal the carbonyl group is replaced by a vinyl group, Figure 1, then the relevant σ/π interactions in 1-butene should be weaker than in propanal because the $\pi^*_{C=C}$ antibonding orbital is a poorer electron acceptor than both carbonyl and thiocarbonyl group.

Figure 5a−c shows plots of the $\sigma_{C_\alpha-H_a} \rightarrow \pi^*_{C_c=X}$, and $\sigma_{C_\alpha-C_\beta} \rightarrow \pi^*_{C_c=X}$ interactions vs θ for thiopropanal (X = S), propanal (X = O), and 1-butene (X = CH_2), respectively. These interactions follow the expected trend, i.e., they decrease along the series from thiopropanal to 1-butene, whereas the angular dependence is similar in all three cases.

The $^3J_{HH}(180°) - {}^3J_{HH}(0°)$ differences for the three model molecules are plotted in Figure 5d−f. They follow qualitatively similar trends and their amplitude decreases notably along this series, paralleling the behavior of σ/π interactions displayed in Figures 5a−c. These results strongly support the hypothesis about the importance played by σ/π interactions in defining the $^3J_{HH}(180°) < {}^3J_{HH}(0°)$ relationship. The plots of $^3J_{HH}(0°)$ and $^3J_{HH}(180°)$ vs θ are shown in Figures 5g−i. Both plots show essentially similar behavior along this series, where differences can be easily rationalized as originating in the two effects discussed above for propanal, i.e., the σ/π hyperconjugative interactions and the proximity effect between the carbonyl and ethyl groups. Along this series, it is interesting to note that the different efficiency of the "activated" coupling pathway for $^3J_{HH}(0°)$ and $^3J_{HH}(180°)$ increases when increasing the σ/π interactions, reinforcing the possibility of obtaining $^3J_{HH}(180°) < {}^3J_{HH}(0°)$ when the molecular fragment **M** shows stronger hyperconjugative interactions with the ethyl group.

4. Conclusions

The origin of the unusual C_1 positive Fourier coefficient, or the anomalous $^3J_{HH}(180°) - {}^3J_{HH}(0°)$ relationship found in some molecules has been studied at the DFT level in three model molecules.

The effects of the substituent and its rotation on $^3J_{HH}(180°)$ and $^3J_{HH}(0°)$ SSCC have been investigated at B3LYP level and with the TZVP basis set after checking that these results are similar to those of ab initio levels (SOPPA and CCSD(SOPPA)) and to those of larger basis sets (EPR-III, aug-cc-pVTZ, and BS2).

It is concluded that strong hyperconjugative interactions involving both bonding and antibonding orbitals of the coupling pathway as well as of the carbonyl group are essential to explain the "anomalous" behavior of $^3J_{HH}$. Such interactions define an additional coupling pathway for $^3J_{HH}$. For propanal, this additional pathway partially can be assigned to simultaneous σ/π hyperconjugative interactions $\sigma_{C_\alpha-H_a} \rightarrow \pi^*_{C_c=X}$, and $\sigma_{C_\alpha-C_\beta} \rightarrow \pi^*_{C_c=X}$ (X = O). These interactions are more efficient for $^3J_{HH}(0°)$ than for $^3J_{HH}(180°)$. Moreover, for θ angles where these interactions are strongest, the $^3J_{HH}(0°)$ couplings are larger than $^3J_{HH}(180°)$ and the C_1 coefficient becomes positive.

Analogous interactions have been detected in thiopropanal (X = S) and 1-butene (X = CH_2). In the former, the hyperconjugative effects are stronger than in propanal because of a better electron acceptor behavior of the $\pi^*_{S=C}$ antibonding orbital, whereas in butane, the weaker effect is attributed to the poorer electron acceptor behavior of the $\pi^*_{C=C}$ antibonding orbital.

Acknowledgment. R.H.C. gratefully acknowledges economic support from UBACYT (X222) and CONICET (PIP 5119/05). R.S. and R.C.O. acknowledge a research fellowship from Universidad Autónoma de Madrid. J.M.G.V. and J.S.F. gratefully acknowledge the financial support from the Dirección General de Enseñanza Superior e Investigación Científica of Spain (DGESIC, projects CTQ2005-04469, CTQ2007-63332, and CTQ2007-66547). Computer time has been partially provided by the Centro de Computación Científica of Universidad Autónoma de Madrid.

References

(1) (a) Karplus, M. *J. Chem. Phys.* **1959**, *30*, 11. (b) Karplus, M. *J. Phys. Chem.* **1960**, 1793. (c) Karplus, M. *J. Am. Chem. Soc.* **1963**, *85*, 2870.

(2) (a) Bystrov, V. F. *Prog. NMR Spectrosc.* **1976**, *10*, 41. (b) Haasnoot, C. A. G.; De Leeuw, F. A. A. M.; Altona, C. *Tetrahedron* **1980**, *36*, 2783. (c) Imai, K.; Osawa, E. *Magn. Reson. Chem.* **1990**, *28*, 668. (d) Altona, C.; Ippel, J. H.; Hoekzema, A. J. A. W.; Erkelens, C.; Groesbeek, M.; Donders, L. A. *Magn. Reson. Chem.* **1989**, *27*, 564. (e) Díez, E.; San Fabián, J.; Guilleme, J.; Altona, C.; Donders, L. A. *Mol. Phys.* **1989**, *68*, 49.

(3) Rule, G. S. Hitchens, T. K. Protein Structure Determination. In *Fundamentals of Protein NMR Spectroscopy*; Springer: Dordrecht, The Netherlands, 2006; p 387.

(4) Suardíaz, R.; Pérez, C.; García de la Vega, J. M.; San Fabián, J.; Contreras, R. H. *Chem. Phys. Lett.* **2007**, *442*, 119.

(5) Pérez, C.; Löhr, F.; Rüterjans, H.; Schmidt, J. M. *J. Am. Chem. Soc.* **2001**, *123*, 7081.

(6) Chou, J. J.; Case, D. A.; Bax, A. *J. Am. Chem. Soc.* **2003**, *125*, 8959.

(7) Lindorff-Larsen, K.; Best, R. B.; Vendruscolo, M. *J. Biomol. NMR* **2005**, *32*, 273.

(8) Juranic, N.; Atanasova, E.; Moncrieffe, M. C.; Prendergast, F. G.; Macura, S. *J. Magn. Reson.* **2005**, *175*, 222.

(9) Case, D. A.; Scheurer, C.; Brüschweiller, R. *J. Am. Chem. Soc.* **2000**, *122*, 10390.

(10) (a) Munzarová, M. L.; Sklenár, V. *J. Am. Chem. Soc.* **2002**, *124*, 10666. (b) Munzarová, M. L.; Sklenár, V. *J. Am. Chem. Soc.* **2003**, *125*, 3649.

(11) Barfield, M.; Chakrabarti, B. *Chem. Rev.* **1969**, *69*, 757.

(12) Castillo, N.; Matta, C. F.; Boyd, R. J. *J. Chem. Inf. Model.* **2005**, *45*, 354.

(13) Soncini, A.; Lazzeretti, P. *J. Chem. Phys.* **2003**, *119*, 1343.

(14) (a) Reed, A. E.; Curtiss, L. A.; Weinhold, F. *Chem. Rev.* **1988**, *88*, 899. (b) Weinhold, F. Natural Bond Orbital Methods. In *Encyclopedia of Computational Chemistry*; Schleyer, P. v. R., Allinger, N. L., Clark, T., Gasteiger, J., Kollman, P. A., Schaefer, H. F., III, Schreiner, P. R., Eds.; John Wiley & Sons: Chichester, U.K., 1998; Vol. 3, p 1792.

(15) Contreras, R. H.; Esteban, A. L.; Díez, E.; Head, N. J.; Della, E. W. *Mol. Phys.* **2006**, *104*, 485.

(16) Tormena, C. F.; Rittner, R.; Contreras, R. H.; Peralta, J. E. *J. Phys. Chem. A* **2004**, *108*, 7762.

(17) Contreras, R. H.; Esteban, A. L.; Díez, E.; Della, E. W.; Lochert, I. J.; dos Santos, F. P.; Tormena, C. F. *J. Phys. Chem. A* **2006**, *110*, 4266.

(18) Esteban, A. L.; Galache, M. P.; Mora, F.; Díez, E.; Casanueva, J.; San Fabián, J.; Barone, V.; Peralta, J. E.; Contreras, R. H. *J. Phys. Chem. A* **2001**, *105*, 5298.

(19) dos Santos, F. P.; Tormena, C. F.; Contreras, R. H.; Rittner, R.; Magalhaes, A. *Magn. Reson. Chem.* **2008**, *46*, 107.

(20) Pople, J. A.; Gordon, M. *J. Am. Chem. Soc.* **1967**, *89*, 4253.

(21) Hermosilla, L.; Calle, P.; García de la Vega, J. M.; Sieiro, C. *J. Phys. Chem. A* **2005**, *109*, 1114.

(22) Frisch, M. J.; Trucks, G. W.; Schlegel, H. B.; Scuseria, G. E.; Robb, M. A.; Cheeseman, J. R.; Montgomery, Jr., J. A.; Vreven, T.; Kudin, K. N.; Burant, J. C.; Millam, J. M.; Iyengar, S. S.; Tomasi, J.; Barone, V.; Mennucci, B.; Cossi, M.; Scalmani, G.; Rega, N.; Petersson, G. A.; Nakatsuji, H.; Hada, M.; Ehara, M.; Toyota, K.; Fukuda, R.; Hasegawa, J.; Ishida, M.; Nakajima, T.; Honda, Y.; Kitao, O.; Nakai, H.; Klene, M.; Li, X.; Knox, J. E.; Hratchian, H. P.; Cross, J. B.; Bakken, V.; Adamo, C.; Jaramillo, J.; Gomperts, R.; Stratmann, R. E.; Yazyev, O.; Austin, A. J.; Cammi, R.; Pomelli, C.; Ochterski, J. W.; Ayala, P. Y.; Morokuma, K.; Voth, G. A.; Salvador, P.; Dannenberg, J. J.; Zakrzewski, V. G.; Dapprich, S.; Daniels, A. D.; Strain, M. C.; Farkas, O.; Malick, D. K.; Rabuck, A. D.; Raghavachari, K.; Foresman, J. B.; Ortiz, J. V.; Cui, Q.; Baboul, A. G.; Clifford, S.; Cioslowski, J.; Stefanov, B. B.; Liu, G.; Liashenko, A.; Piskorz, P.; Komaromi, I.; Martin, R. L.; Fox, D. J.; Keith, T.; Al-Laham, M. A.; Peng, C. Y.; Nanayakkara, A.; Challacombe, M.; Gill, P. M. W.; Johnson, B.; Chen, W.; Wong, M. W.; Gonzalez C.; Pople J. A. *Gaussian 03, Revision D.01*; Gaussian, Inc.: Wallingford, CT, 2004.

(23) Helgaker, T.; Aa. Jensen, H. J.; Jorgensen, P.; Olsen, J.; Ruud, K.; Agreni, H.; Andersen, T.; Bak, K. L.; Bakken, V.; Christiansen, O.; Dahle, P.; Dalskov, E. K.; Enevoldsen, T.; Fernandez, B.; Heibergi, H.; Hettema, H.: Jonsson, D.; Kirpekar, S.; Kobayashi, R.; Koch, H.; Mikkelsen, K. V.; Norman, P.; Packer, M. J.; Saue, T.; Taylor, P. R.; Vahtras, O. Dalton, An Electronic Structure Program, releases 1.2; University of Oslo: Oslo, Norway, 1997.

(24) Glendening, E. D.; Reed, A. E.; Carpenter, J. E.; Weinhold, F. *Gaussian NBO, version 3.1*; Gaussian Inc.: Pittsburgh, PA.

(25) Suardíaz, R.; Pérez, C.; Crespo-Otero.; García de la Vega, J. M.; San Fabián, J. *J. Chem. Theory Comput.* **2008**, *4*, 448.

(26) Guilleme, J.; San Fabián., J.; Casanueva, J.; Díez, E. *Chem. Phys. Lett.* **1999**, *314*, 168.

CT800145H